

See discussions, stats, and author profiles for this publication at: <https://www.researchgate.net/publication/292688765>

# Finite element solution of radiative heat transfer in a rectangular enclosure with participating media

Article · November 2004

CITATIONS

2

READS

114

3 authors, including:



Hong Qi

Harbin Institute of Technology

181 PUBLICATIONS 1,429 CITATIONS

SEE PROFILE

Some of the authors of this publication are also working on these related projects:



Near field radiative heat transfer [View project](#)



Inverse heat transfer problem [View project](#)

## **Development of a Finite Element Radiation Model Applied to Two-Dimensional Participating Media**

Hong Qi, Liming Ruan, and Jianyu Tan

School of Energy Science and Engineering, Harbin Institute of Technology, Harbin 150001,  
People's Republic of China

A finite element method (FEM) for radiative heat transfer has been developed and it is applied to 2D problems with unstructured meshes. The present work provides a solution for temperature distribution in a rectangular enclosure with black or gray walls containing an absorbing, emitting, isotropically scattering medium. Compared with the results available from Monte Carlo simulation and finite volume method (FVM), the present FEM can predict the radiative heat transfer accurately. © 2005 Wiley Periodicals, Inc. *Heat Trans Asian Res*, 34(6): 386–395, 2005; Published online in Wiley InterScience (www.interscience.wiley.com). DOI 10.1002/htj.20076

**Key words:** finite element method, radiative heat transfer, unstructured meshes, participating media

### **1. Introduction**

Radiative heat transfer is a major heat transfer model and it is usually strongly coupled with fluid dynamics in many high-temperature systems such as boilers, furnaces, rocket engines, etc. An accurate modeling of these systems requires a simultaneous solution of the radiative transfer equation (RTE) and the fluid dynamics equations. In the last several decades, many methods have been developed for solving the RTE. They include the zone method, Monte Carlo method, flux method, discrete transfer method, P-N method, discrete ordinates method (DOM), finite volume method (FVM), etc. Each of these methods has its own relative advantages and disadvantages and none of them is superior to the others in all aspects. However, many numerical complications may arise from incompatibilities between the radiative transport model and the discrete formulation employed for fluid dynamics and other heat transfer modes. The finite element formulation for RTE avoids many of these complications and has the advantage of greater compatibility with existing finite element based heat transfer software. Besides, the FEM could simplify the problems of complex geometries using unstructured meshes.

---

Contract grant sponsor: National Natural Science Foundation of China (No. 50276014).

Since the first applications of the FEM to radiative transport in the early 1980s, however, the speed and memory capacity of computer hardware has increased dramatically and promises to continue to do so in the future. With these points in mind, the continued development of the FEM for radiative transport applications is warranted. Reddy and Murty (1978) [1] provide one of the earliest applications of the FEM to radiative transport. This work considers the solution of integral equations peculiar to two one-dimensional radiative transport problems using the FEM and do not include other heat transport modes. A series of articles in the early 1980s consider the solution of one-dimensional conduction and radiation problems. The work of Wu et al. [2] (1980) and Fernandes et al. [3] (1980) considered 1D plane conduction and radiation problem. Fernandes et al. [4] (1982) extended the one-dimensional plane formulation of the earlier work to cylindrical coordinates. This later work also includes isotropic scattering. The most significant work involving combined convection, conduction, and radiation heat transfer is provided by Chung et al. [5] (1984) and Utreja et al. [6] (1989). The work of Brandon and Derby [7, 8] (1991, 1992) employs the approximation in a finite element formulation of a two-dimensional axisymmetric, nonscattering combined mode problem. They also suggest various techniques to reduce computational overhead in the evaluation of radiation integrals. More recently, Piotr et al. [9] (2004) proposes a FEM to calculate temperature, conductive and radiative heat flux distributions in a participating medium.

The objective of this study is to develop an accurate and efficient radiation model applicable for 2D planar geometry using an unstructured meshes finite element method. Compared with the results available of Monte Carlo simulation (M-C) and finite volume method (FVM), the present FEM can accurately predict the radiation transfer.

### Nomenclature

$A$ :	area
$H^1$ :	Hilbert space of functions with continuous first derivatives
$H^{1(N)}$ :	$N$ dimensional finite subspace spanned by the set of finite element basis functions
$I$ :	mean incident intensity
$\mathbf{n}$ :	outward directed unit surface normal vector at the domain boundary
$n$ :	number of nodes in the finite element mesh
$N$ :	finite element basis function
$q$ :	heat flux
$q^*$ :	dimensionless heat flux $q^* = q/\sigma T_g^4$
$\mathbf{q}_r$ :	radiative flux vector
$\mathbf{r}$ :	three-dimensional relative position vector
$\mathbf{r}_*$ :	position of point *
$\hat{\mathbf{r}}$ :	unit vector of position vector $\hat{\mathbf{r}} = \mathbf{r}/ \mathbf{r} $
$\mathbf{r}_{i*}$ :	relative position between points $i$ and $*$ , $\mathbf{r}_i^* = \mathbf{r}_i - \mathbf{r}_*$
$S_n(x)$ :	two-dimensional exponential integral function
$T$ :	temperature
$V$ :	volume
$x, y$ :	principal Cartesian coordinate directions

## Greek Symbols

$\partial\Omega$ :	domain boundary
$\varepsilon$ :	surface emissivity
$\kappa$ :	extinction coefficient $\kappa = \kappa_a + \kappa_s$
$\kappa_a$ :	absorption coefficient
$\kappa_s$ :	scattering coefficient
$\sigma$ :	Stefan–Boltzmann constant, $5.670 \times 10^{-8} \text{ W} \cdot \text{m}^{-2} \cdot \text{K}^{-4}$
$\Phi$ :	scattering phase function
$\Omega$ :	computational domain $\Omega \subset R^n$
$\omega$ :	single-scattering albedo

## Subscripts and Superscript

$*$ :	dummy integration variables
$i, j, k$	nodal indices

## 2. Numerical Model

Usually the transient term in radiative energy conservation equation is neglected. The governing heat transport equation takes the form:

$$\nabla \cdot \mathbf{q}_r(\mathbf{r}) = 0 \quad (1)$$

$$\nabla \cdot \mathbf{q}_r(\mathbf{r}) = 4\pi\kappa_a \left[ \frac{\sigma T^4(\mathbf{r})}{\pi} - I(\mathbf{r}) \right] \quad (2)$$

where  $\nabla \cdot \mathbf{q}_r(\mathbf{r})$  is the divergence of the radiative heat flux, which represents the difference between the energy emitted from a point through thermal radiation and the incident energy from all other points in the domain.  $I(\mathbf{r})$  is the mean incident intensity at location  $\mathbf{r}$  and represents the average incident intensity at a given point in the region of interest as well as reflection and emission from the boundary of the region. For a gray, isotropically scattering medium, the mean intensity at location is given by Lin [10] (1988):

$$\begin{aligned} I(\mathbf{r}_i) = & \frac{1}{4\pi} \left\{ -\frac{1}{\pi} \int_{\partial\Omega} (1 - \varepsilon)(\mathbf{q}_r(\mathbf{r}_*) \cdot \mathbf{n}) \frac{[\mathbf{n} \cdot \mathbf{r}_i^*]}{|\mathbf{r}_i^*|^2} \exp(-\kappa|\mathbf{r}_i^*|) dA_* \right. \\ & - \frac{1}{\pi} \int_{\partial\Omega} \varepsilon \sigma T^4(\mathbf{r}_*) \frac{[\mathbf{n} \cdot \mathbf{r}_i^*]}{|\mathbf{r}_i^*|^2} \exp(-\kappa|\mathbf{r}_i^*|) dA_* + \\ & \left. \frac{1}{\pi} \int_{\Omega} \kappa_a \sigma T^4(\mathbf{r}_*) \frac{\exp(-\kappa|\mathbf{r}_i^*|)}{|\mathbf{r}_i^*|^2} dV_* + \int_{\Omega} \kappa_s I(\mathbf{r}_*) \frac{\exp(-\kappa|\mathbf{r}_i^*|)}{|\mathbf{r}_i^*|^2} dV_* \right\} \quad (3) \end{aligned}$$

The first two integrals in Eq. (3) represent diffuse reflection and emission from the boundaries of the region. The third and fourth integrals in Eq. (3) represent the influence of volumetric emission

and isotropic scattering at all other points in the domain on the incident intensity at point  $\mathbf{r}_i$ . Here, we assume the physical parameters of the medium are uniform. The exponential terms in each of the integrals represents the attenuation of radiation between location  $\mathbf{r}_*$  and the interest point  $\mathbf{r}_i$ , where  $\kappa$  is the extinction coefficient,  $\kappa = \kappa_a + \kappa_s$ , and  $\mathbf{r}_i^*$  is the relative position vector given by  $\mathbf{r}_i^* = \mathbf{r}_i - \mathbf{r}_*$ .  $\mathbf{q}_r(\mathbf{r}_*)$  is the radiative heat flux vector at point  $\mathbf{r}_i$  which is given by an expression similar to Eq. (3):

$$\begin{aligned} \mathbf{q}_r(\mathbf{r}_i) = & \frac{1}{\pi} \int_{\partial\Omega} (1 - \epsilon)(\mathbf{q}_r(\mathbf{r}_*) \cdot \mathbf{n})[\mathbf{n} \cdot \mathbf{r}_i^*] \cdot \frac{\hat{\mathbf{r}}_i^*}{|\mathbf{r}_i^*|^2} \exp(-\kappa|\mathbf{r}_i^*|) dA_* \\ & - \frac{1}{\pi} \int_{\partial\Omega} \epsilon \sigma T^4(\mathbf{r}_*)[\mathbf{n} \cdot \mathbf{r}_i^*] \cdot \frac{\hat{\mathbf{r}}_i^*}{|\mathbf{r}_i^*|^2} \exp(-\kappa|\mathbf{r}_i^*|) dA_* + \\ & - \frac{1}{\pi} \int_{\Omega} \kappa_a \sigma T^4(\mathbf{r}_*) \frac{\hat{\mathbf{r}}_i^*}{|\mathbf{r}_i^*|^2} \exp(-\kappa|\mathbf{r}_i^*|) dV_* + \int_{\Omega} \kappa_s I(\mathbf{r}_*) \frac{\hat{\mathbf{r}}_i^*}{|\mathbf{r}_i^*|^2} \exp(-\kappa|\mathbf{r}_i^*|) dV_* \end{aligned} \quad (4)$$

$\mathbf{n}$  is the outward directed unit surface normal vector at the domain boundary  $\mathbf{r}_*$ .  $T(\mathbf{r}_*)$  is the temperature of the differential volume  $dV_*$  at  $\mathbf{r}_*$ .

### 3. Solution and Discussion

The principal approximation of the finite element formulation is the Galerkin approximation which restricts the solution to a finite subspace of the Hilbert space,  $H^{1(N)}$ , which is spanned by a set of basis vectors or functions  $N(x)$ . In the simulation procedure by FEM, each of the unknowns in Eqs. (3) and (4) may be expressed in terms of a linear combination of the finite element basis functions. Here the finite element formulation is simplified considerably by employing the Swartz–Wendroff approximation [7, 8]:

$$T(\mathbf{r}) = \sum_{j=1}^n T_j N_j(\mathbf{r}) \quad I(\mathbf{r}) = \sum_{j=1}^n I_j N_j(\mathbf{r}) \quad T^4(\mathbf{r}) = \sum_{j=1}^n T_j^4 N_j(\mathbf{r}) \quad (5)$$

By substituting the basis expansions for the mean incident intensity and the fourth power of the temperature into Eq. (3) and Eq. (4), the following compact form of discrete equations for the nodal mean incident intensity may be obtained:

$$I_i = \frac{1}{4\pi} \left\{ - (1 - \epsilon) \mathbf{q}_{r,j} \cdot \mathbf{R} i_{ij} - T_j^4 \left[ \sigma \epsilon E i_{ij} - \left( \frac{\kappa_a \sigma}{\pi} \right) S i_{ij} \right] + \kappa_s I_j S i_{ij} \right\} \quad (6)$$

where  $E i_{ij}$ ,  $R i_{ij}$ , and  $S i_{ij}$  are the compact integral factors. By examining the equations, it becomes evident that, as long as the assumption of constant medium properties holds, the integral factors do not depend on the solution itself and may be evaluated once and stored in memory. The factors are defined as follows:

$$Ei_{ij} = \int_{\partial\Omega} N_j \frac{[\mathbf{n} \cdot \mathbf{r}_i^*]}{|\mathbf{r}_i^*|} S_2(-\kappa|\mathbf{r}_i^*|) dA_* \quad (7)$$

$$Ri_{ij} = \int_{\partial\Omega} N_j \frac{[\mathbf{n} \cdot \mathbf{r}_i^*]}{|\mathbf{r}_i^*|} S_2(-\kappa|\mathbf{r}_i^*|) \cdot \mathbf{n} dA_* \quad (8)$$

$$Si_{ij} = \pi \int_{\Omega} N_j \frac{S_1(-\kappa|\mathbf{r}_i^*|)}{|\mathbf{r}_i^*|} dV_* \quad (9)$$

$S_n(x)$  is given as follows:

$$S_n(x) = \frac{2}{\pi} \int_0^{\pi/2} \exp(x \sec \theta) \cos^{n-1} \theta d\theta \quad (10)$$

A similar expression for the radiative heat flux vector may also be obtained:

$$\mathbf{q}_{r,i} = -(1 - \varepsilon) \mathbf{q}_{r,j} \cdot Rq_{ij} - T_j^4 \left[ \sigma \varepsilon E q_{ij} - \left( \frac{\kappa_a \sigma}{\pi} \right) S q_{ij} \right] + \kappa_s I_j S q_{ij} \quad (11)$$

where  $E q_{ij}$ ,  $R q_{ij}$ , and  $S q_{ij}$  are the compact integral factors:

$$E q_{ij} = \int_{\partial\Omega} N_j \frac{\hat{\mathbf{r}}_i^*}{|\mathbf{r}_i^*|} S_3(-\kappa|\mathbf{r}_i^*|) \cdot [\mathbf{n} \cdot \mathbf{r}_i^*] dA_* \quad (12)$$

$$R q_{ij} = \int_{\partial\Omega} N_j \frac{\hat{\mathbf{r}}_i^*}{|\mathbf{r}_i^*|} S_3(-\kappa|\mathbf{r}_i^*|) \cdot [\mathbf{n} \cdot \mathbf{r}_i^*] dA_* \quad (13)$$

$$S q_{ij} = \pi \int_{\Omega} N_j \frac{\hat{\mathbf{r}}_i^*}{|\mathbf{r}_i^*|} S_2(-\kappa|\mathbf{r}_i^*|) dV_* \quad (14)$$

In this study, by the Galerkin translation, the weak form of the energy Eq. (1) is derived by setting the inner product of the residual vector with each of the basis functions  $N_i$  equal to zero. Meanwhile, the fourth power of the temperature in the control Eq. (2) is expanded by the Taylor series  $T_j^4 = 4T_j^{*3}T_j - 3T_j^{*4}$ , where  $T_j^*$  is assumed to be the temperature value of previous iteration (the initial value is guessed). This results in  $N$  simultaneous equations that are similar to those in Eq. (2) with the weight function  $N_i$ :

$$(4T_j^{*3}T_j - 3T_j^{*4}) \int_{\Omega} N_i N_j d\Omega - I_j \int_{\Omega} N_i N_j d\Omega = 0 \quad (15)$$

Note that the energy conservation equation and the radiative transport equation should be simulated by FEM simultaneously. In order to get the accurate results with less time consumption, the following key aspects should be focused on

1) Discrete procedure of the radiative transfer equation. By assuming the nodal temperature, the nodal mean incident intensity  $I(\mathbf{r})$  is evaluated from RTE, then  $I(\mathbf{r})$  is substituted directly into the energy equation as the initial value to evaluate the temperature distribution through the iterative solution.

2) Selection of a suitable method to solve the linear equations. Since the coefficient matrix of the equations may occur non-positive, the Gauss–Jordan elimination method is selected. Meanwhile, since the coefficient matrix is a big sparse symmetric matrix, a new one-dimensional array storage technique is used to save memory.

3) Selection of the integral method. In this study, the low-order Gauss–Legendre integration provides sufficient accuracy for all the other elements not in the near field of node  $i$ . For  $|\mathbf{r}_i| \rightarrow 0$ , the ten point integration rule is used without being excessively expensive.

4) Treatment of the boundary condition. For the pure radiative heat transfer model, there is a temperature discontinuity between the boundary and the media. The temperature value is not identical at the same node point. For the first type of boundary conditions, the boundary nodal temperature values of the wall are given. However, considering the temperature discontinuity, the boundary nodal temperature value of media is not fixed in every iterative procedure.

### 3.1 The radiative transfer in a rectangular medium

The present case provides a solution for the temperature distribution in a rectangular enclosure (1 m  $\times$  1 m) with black or gray walls containing an absorbing, emitting, isotropically scattering medium. The three points of triangle element and four points of quadrilateral element are used respectively.

#### Case 1

The physical model is as follows:  $\varepsilon = 1.0$ ,  $\kappa_e = 2.0 \text{ m}^{-1}$ ,  $\omega = 0.5$ . The temperature of the left side and right surface are 1000 K and 500 K, respectively. The temperature distribution of the top and bottom surface is  $T = 1000 - 500x$  (K) along the  $x$  axis. The temperature of the medium is shown in Fig. 1.

Table 1 shows the comparison of temperature distribution along the  $x$  axis at  $y = 0.7727$  m by FEM with unstructured element and MC [11] simulation with meshes  $31 \times 31$ . Three cases with different element numbers (1404, 1864, and 2482) are selected to analyze the performance of FEM. As noted in Table 1, the maximum relative errors are about 2.54%, 2.34%, and 0.48%. It indicates that our FEM simulation could accurately predict the radiation transfer.

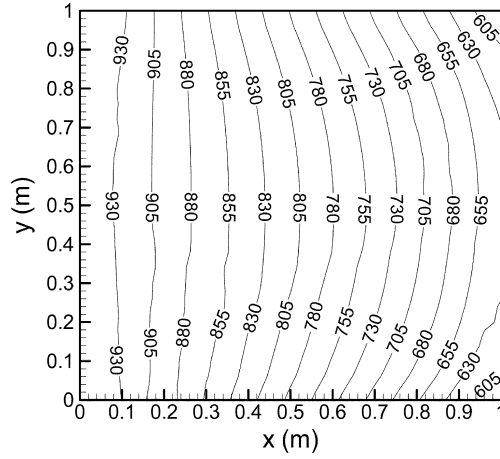


Fig. 1. The temperature distribution with black boundary (1404 elements).

## Case 2

The boundary surface is assumed to be gray with  $\epsilon = 0.2$ ,  $\epsilon = 0.5$ , and  $\epsilon = 0.8$ , respectively. The other parameters are the same and the temperature distribution is shown in Fig. 2.

As noted in Figs. 1 and 2, with the decrease of the boundary emissivity (the increase of the boundary reflectivity), the temperature distribution trends to be more uniform. The reason is that the emission power is proportional to the emissivity of the boundary wall for the first kind of the boundary condition. For the gray boundary, the radiative energy is reflected partially to the medium, which

Table 1. Comparison of Results by FEM and M-C Simulation (along  $y = 0.7727$  m)

node	$x$	MC	FEM (element number)		
			1404	1864	2482
1	0.3387	865.6475	854.7229	856.2353	869.7896
2	0.3710	856.8124	844.5250	845.2099	860.0104
3	0.4032	847.4986	834.1766	833.1461	850.1842
4	0.4355	838.4952	823.6863	823.1783	840.2021
5	0.4677	828.9630	813.1438	813.1833	830.1548
6	0.5000	819.5942	802.5206	802.2334	819.8879
7	0.5323	809.8014	791.8106	791.7998	809.3813
8	0.5645	799.9530	781.0081	781.2143	798.4063
9	0.5968	790.1042	770.0675	771.5645	787.9439



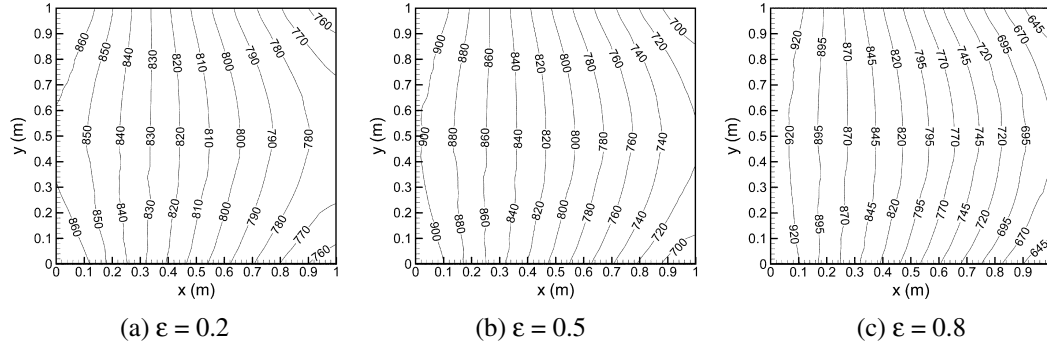


Fig. 2. The temperature distribution of gray boundary with different emissivity (1404 elements).

make the temperature distribution of the media become more uniform. Given an increase of the boundary reflectivity, the temperature distribution of the media becomes more and more uniform and the temperature gradient decreases gradually.

### 3.2 The radiative transfer in irregular 2D media

Reference 12 calculated the dimensionless heat flux  $q^*$  of an irregular quadrilateral enclosure without scattering by the FVM. In the present study, the FEM is used to solve the same problem with meshes  $10 \times 10$  (as shown in Fig. 3). The temperature of the media is  $T_g$  and the boundary is a black wall with 0 K. The absorption coefficient is given as  $0.1 \text{ m}^{-1}$ ,  $1.0 \text{ m}^{-1}$ , and  $10 \text{ m}^{-1}$ , respectively. The results are shown in Fig. 4. It validates that the present FEM simulation could accurately predict the radiation transfer in irregular 2D enclosure.

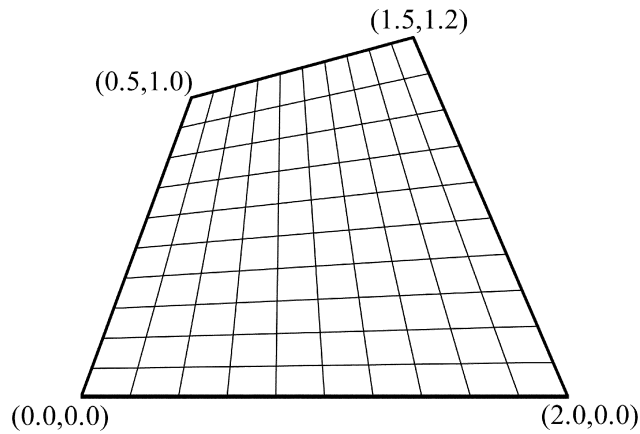


Fig. 3. Computation grid of the irregular quadrilateral enclosure.

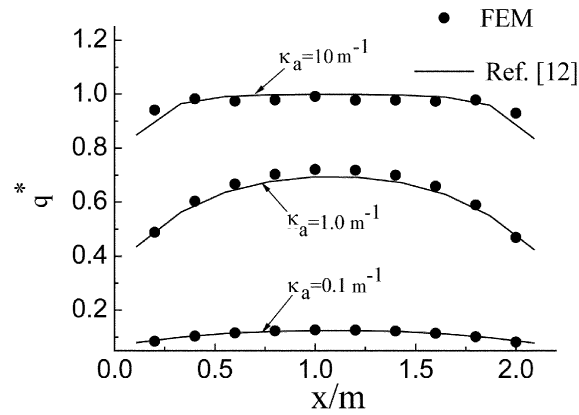


Fig. 4. Dimensionless fluxes on the bottom wall.

#### 4. Conclusions

In the present study, an unstructured finite element method (FEM) for radiative heat transfer has been developed and it is applied for 2D problems. The present work provides a solution for temperature distribution in a rectangular enclosure with black or gray walls containing an absorbing, emitting, isotropically scattering medium. Compared with the available results of Monte Carlo simulation and FVM, the present FEM could not only predict the radiation transfer accurately and efficiently but is also flexible in treating problems with complicated geometries. As the finite element formulation for RTE has the advantage of greater compatibility with the discrete formulation employed for fluid dynamics and other heat transfer modes, the continued development of the FEM for radiative transport applications in 3D problems will be studied in the future.

#### Acknowledgments

The support of this work by the National Natural Science Foundation of China (No. 50276014) is gratefully acknowledged.

#### Literature Cited

1. Reddy JN, Murty VD. Finite element solution of integral equations arising in radiative heat transfer and laminar boundary layer theory. *Numerical Heat Transfer* 1978;1:389–401.
2. Wu ST, Ferguson RE, Altgibers LL. Application of finite element techniques to the interaction of conduction and radiation in participating medium. *Heat Transfer and Thermal Control, Progress in Astronautics and Aeronautics*, AIAA 1980;78:61–91.
3. Fernandes RL, Francis J, Reddy JN. A finite-element approach to combined conductive and radiative heat transfer in a planar medium. *Heat Transfer and Thermal Control, Progress in Astronautics and Aeronautics*, AIAA 1980;78:91–109.
4. Fernandes RL, Francis J. Combined conductive and radiative heat transfer in an absorbing, emitting, and scattering cylindrical medium. *J Heat Transfer Trans ASME* 1982;104:594–601.
5. Chung TJ, Kim JY. Two-dimensional, combined-modes heat transfer by conduction, convection, and radiation in emitting, absorbing and scattering media-solution by finite elements. *J Heat Transfer Trans ASME* 1984;106:448–452.

6. Utreja LR, Chung TJ. Combined convection-conduction-radiation boundary layer flows using optimal control penalty finite elements. *J Heat Transfer Trans ASME* 1989;111:433–437.
7. Brandon S, Derby JJ. A finite element method for internal radiative heat transfer and its application to analysis of the growth of semitransparent crystals. *Fundamentals of Radiation Heat Transfer*, ASME HTD 1991;106:1–16.
8. Brandon S, Derby JJ. A finite element method for conduction internal radiation and solidification in a finite axisymmetric enclosure. *Fundamentals of Radiation Heat Transfer*, ASME HTD 1992;106:1–16.
9. Piotr F, Jerzy B. Finite element analysis of concurrent radiation and conduction in participating media. *JQSRT* 2004;84:563–573.
10. Lin JD. Radiative transfer within an arbitrary isotropically scattering medium enclosed by diffuse surfaces. *J Thermophys Heat Transfer* 1988;2:68–74.
11. Ruan LM, Tan HP, Yan YY. A Monte-Carlo (MC) method applied to the medium with non-gray absorbing-emitting-anisotropic scattering particles and gray approximation. *Numerical Heat Transfer Part A: Application* 2002;42:253–268.
12. Chai JC, Parthasarathy G, Lee HS, Patankar SV. Finite volume radiative heat transfer procedure for irregular geometries. *J Thermophys Heat Transfer AIAA* 1995;9:410–415.



Originally published in *Chinese Journal of Computational Physics* **21**, 2004, 547–550.

Translated by Hong Qi, School of Energy Science and Engineering, Harbin Institute of Technology,  
and Liming Ruan, School of Energy Science and Engineering, Harbin Institute of Technology,  
92, West Dazhi Street, Harbin 150001, P.R. China.